SIMULATION OF THE SHOT-NOISE DRIVEN MICROBUNCHING INSTABILITY EXPERIMENT AT THE LCLS *

J. Qiang#, LBNL, Berkeley, CA, U.S.A.
Y. Ding, P. Emma, Z. Huang, D. Ratner, T. Raubenheimer, F. Zhou, SLAC, Menlo Park, CA, U.S.A.

Abstract

The shot-noise driven microbunching instability can significantly degrade electron beam quality in next generation light sources. Experiments were carried out at the Linac Coherent Light Source (LCLS) to study this instability. In this paper, we will present start-to-end simulations of the shot-noise driven microbunching instability experiment at the LCLS.

INTRODUCTION

The microbunching instability[1-5], seeded by shot noise and driven by collective effects (primarily space-charge), can significantly degrade the quality of the electron beam before it enterstthe FEL undulators. Recently, a series of experiments were carried out at the LCLS to study the microbunching instability [6]. With the help of x-band transverse deflecting cavity (XTCAV), the longitudinal phase space can be imaged at the end of the accelerator revealing the detailed structure arising from the microbunching instability. To better understand these experimental results, we have done start-to-end macroparticle simulations using real number of electrons on a high performance large scale computer. This also provides a validation of the computational model used in the simulation.

COMPUTATIONAL SETUP

All simulations presented in this study were done using a 3D parallel beam dynamics simulation framework IMPACT [7-8]. It includes a time-dependent 3D space-charge code module IMPACT-T to simulate photo-electron beam generation and acceleration through the s-band photo RF gunand a traveling wave boosting cavity L0, and a position-dependent 3D space-charge code module to simulate electron beam transport through the traveling wave linac system. Besides the 3D space-charge effects, the simulation also includes coherent synchrotron radiation (CSR) effects through a bending magnet, incoherent synchrotron radiation inside the bending magnet, the longitudinal wakefield of the RF structures, and the longitudinal resistive wall wakefields of the long transport lines. All simulations were done using the real number of electrons (1.1×10^9)for the 180-pC bunch charges, to capture the initial shot noise of the beam, which can have important impact on the final beam quality and FEL performance due to the microbunching instability [9-10]. The total computational time takes about 10 hours on thousands of processors at the NERSC supercomputer center [11].

*Work supported by the Director of the Office of Science of the US Department of Energy under Contract no. DEAC02-05CH11231 and DEAC02-76SF00515.
#jqiang@lbl.gov

SIMULATION RESULTS

Figure 1 shows a schematic plot the LCLS accelerator layout used for the microbunching instability experiment. It consists of a photoinjector (not shown in the plot), a short section of linac (L0) before the laser heater, two bunch compressors and three linac sections. The bunch compressor two (BC2) is used to control the final peak current while the linac section 3 (L3) is used (in this case) to de-accelerate electron beam from 5 GeV down to 4.3 GeV. The simulation starts from the emission of the photo-electrons at the cathode. The real number of electrons (180pC) was used in the simulation to model the

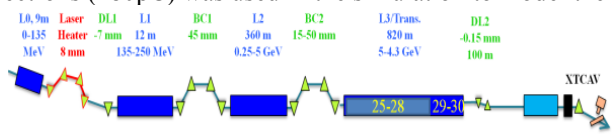

Figure 1: A schematic plot of LCLS accelerator layout.

initial shot-noise of the beam. The initial transverse laser profile is a Gaussian distribution with 1 mm rms size and truncated at 0.5 sigma, the longitudinal profile also has a Gaussian distribution with 1ps rms bunch length and truncated at 2.5 sigma. The initial normalized thermal emittance is about 0.2 um. Figure 2 shows the kinetic energy evolution of the electron beam inside the accelerator. It is accelerated to 250 MeV before bunch compressor one, 5 GeV before bunch compressor two, and de-accelerated down to 4.3 GeV at the end of the accelerator. Figure 3 shows the transverse rms size and the longitudinal rms bunch length evolution through the accelerator. The transverse size is reasonably well matched in the accelerator with less than 100 um rms size. The longitudinal bunch length out of the injector is about 0.5 mm and is compressed to about 0.06 mm after the bunch compressor one and further compressed to about 0.02 mm after the BC2. The compression factor at BC1 is

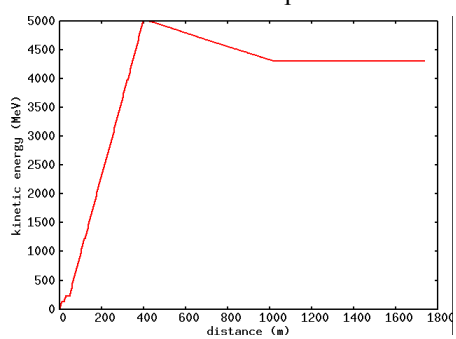

Figure 2: Electron beam kinetic energy evolution through the accelerator.

about 8 and about 3 at BC2. The initial peak current out of the injector is about 35 A. The finial peak current at the end of the accelerator is about 1 kA in one study and500 A in another study.

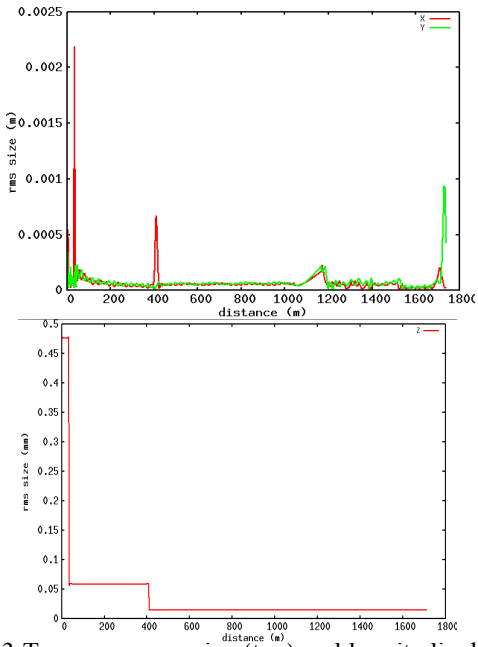

Figure 3:Transverse rms size (top) and longitudinal bunch length (bottom) evolution through the accelerator.

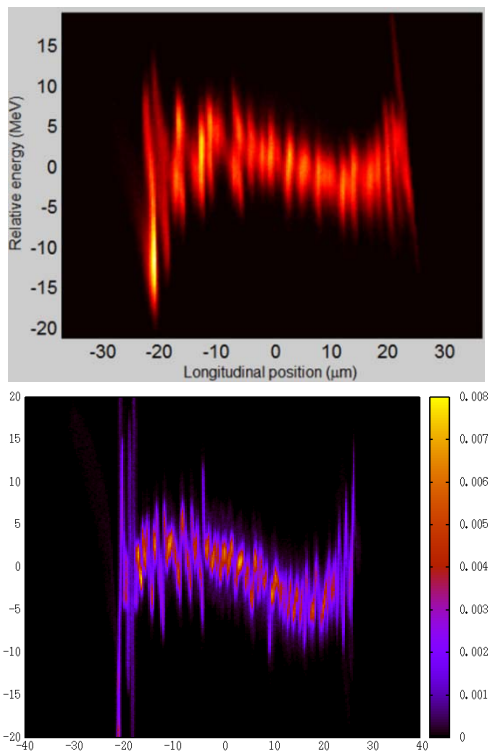

Figure 4: Final longitudinal phase space distribution without using the laser heater from the measurement (top) and from the simulation (bottom) in 1 kA current study.

Figure 4 shows the final longitudinal phase space after the XTCAV from the experimental observation and from the simulation with laser heater turned off for the 1 kA study case (FEL lasing is suppressed here). Here, a strong phase space fluctuation due to the microbunching instability can be seen from both the measurement and the simulation. There is no external seeded initial modulation. This large fluctuation arises from the shot-noise inside the beam and is amplified by collective effects such as space-charge effects through the accelerator. This microbunching instability can be suppressed through Landau damping by increasing the electron beam uncorrelated energy spread before the bunch compressor. A laser heater was built in the LCLS to add uncorrelated energy spread to the beam before BC1. Figure 5shows the final longitudinal phase space after the XTCAV from both the measurement and the simulation with extra 19 keV rms uncorrelated energy spread from the laser heater for the 1 kA case. The phase space fluctuation is significantly reduced with the use of the laser heater. This is observed in both the measurement and the simulation. The simulation also shows similar longitudinal phase space as the measurement. The energy dip around the head of the distribution comes from the effects of resistive wall wakefieldin the long, narrow undulator chamber. The dip near the tail of the distribution is due to the longitudinal space-charge effects from the large current spike near the tail of the electron beam.

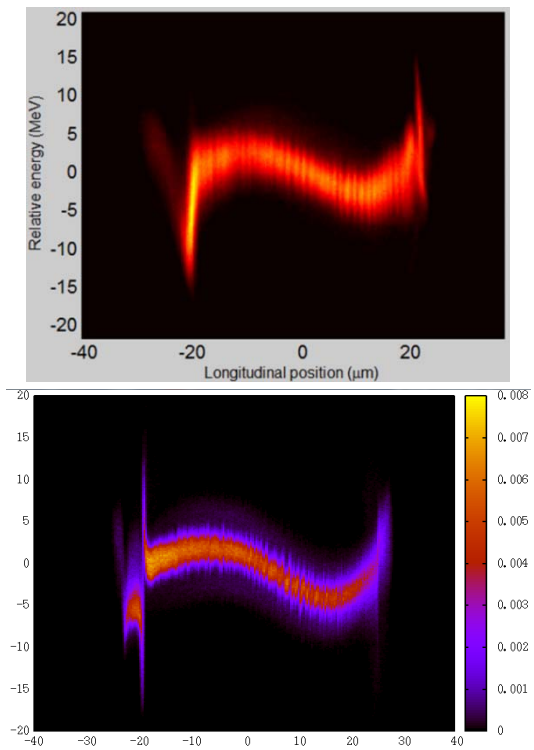

Figure 5: Final longitudinal phase space distribution with extra 19 keV energy spread from the laser heater from the measurement (top) and from the simulation (bottom) in 1 kA current study.

In another study, we also simulated a lower final peak current case (~500 A). Figure 6 shows the final longitudinal phase space from the XTCAV measurement

and from the start-to-end simulation with laser heater turned off. Again, a strong modulation caused by the microbunching instability is observed from both the measurement and the simulation. Figure 7 shows the final longitudinal phases with 19keV extra energy spread from the laser heater. The modulation is reduced significantly in comparison to the zero laser heater setting. The simulation also reproduces the longitudinal phase distribution of the electron beam quite well.

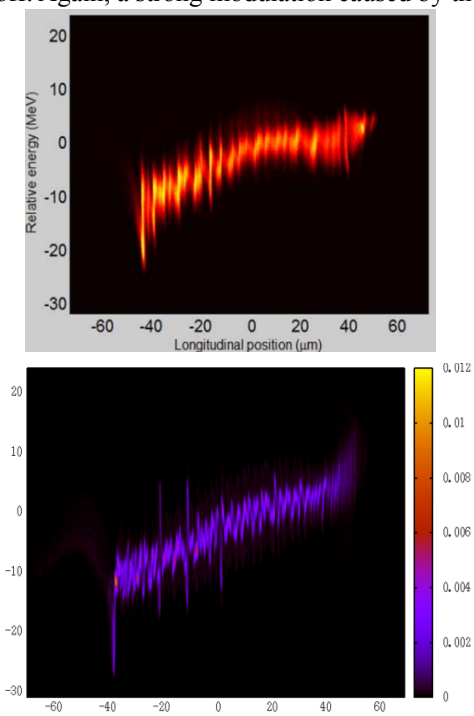

Figure 6: Final longitudinal phase space distribution without using the laser heater from the measurement (top) and from the simulation (bottom) in the 500 A current study.

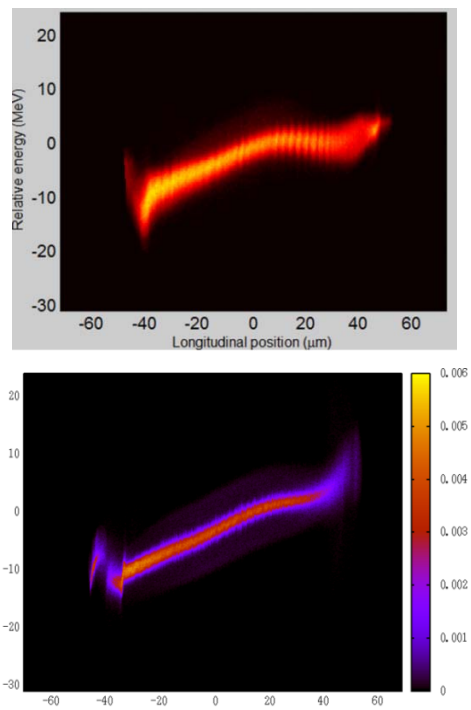

Figure 7: Final longitudinal phase space distribution with 19 keV extra energy spread using the laser heater from the measurement (top) and from the simulation (bottom) in the 500 A current study.

Figure 8 shows the final slice energy spread (SES) after the undulator (FEL off) as a function of the laser heater-induced extra energy spread from both the simulation and the measurement. The simulation results show a similar laser heater induced energy spread dependence to the measured data. Both show the same amount of extra energy spread needed from the laser heater in order to achieve the minimum final slice energy. However, the absolute value of the slice energy spreader from the simulation is smaller than those from the measurement. This will be discussed in the future publication.

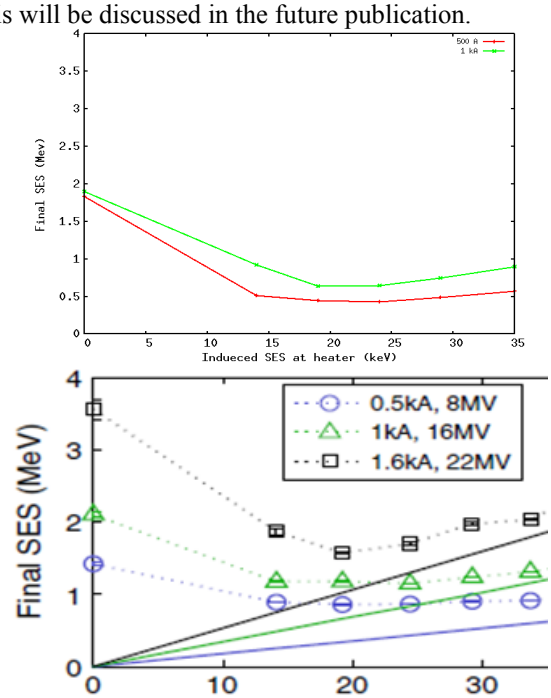

Figure 8: Final slice rms energy spread after the undulatoras a function of laser heater induced extra energy spread. Top plot is simulation while bottom is measurement from Ref. [6].

CONCLUSIONS

In summary, the start-to-end macroparticle simulation using the real number of electrons reproduces the microbunching instability experimental observations at LCLS quite well. The microbunching instability arising from the electron beam shot noise can significantly degrade the final beam quality without the help of the laser heater. The use of laser heater helps mitigate the microbunching instability and drastically reduces final electron phase space fluctuation, which is observed from both the measurement and the simulation. This also helps validate our simulation model and improves ourconfidence in future x-ray light source accelerator design study such as LCLS-II.

REFERENCES

[1] M. Borland *et al., Nucl. Instrum. Methods Phys. Res., Sect. A* vol. 483, p. 268, 2002.
[2] E. L. Saldin, E. A. Schneidmiller, and M. V. Yurkov, *Nucl. Instrum. Methods Phys. Res., Sect.,* vol. 483, p. 516,2002.
[3] S. Heifets, G. Stupakov, and S. Krinsky, *Phys. Rev. ST Accel. Beams,* vol. 5, p. 064401, 2002.
[4] Z. Huang and K. J. Kim, *Phys. Rev. ST Accel. Beams*, vol. 5, 074401, 2002.
[5] Z.Huang *et al., Phys. Rev. ST Accel. Beams,* vol. 7, 074401, 2004.
[6] D. Ratner *et al., Phys. Rev. ST Accel. Beams,* vol. 18, 03070 4, 2015.
[7] J. Qiang *et al., Phys. Rev. ST Accel. Beams,* vol. 9, 044204, 2006.
[8] J. Qiang *et al., J. of Comp. Phys.,* vol. 163, p. 434, 2000.
[9] J. Qiang *et al., Phys. Rev. ST Accel. Beams,* vol. 12, 100702, 2009.
[10] J. Qiang *et al., Phys. Rev. ST Accel. Beams,* vol. 17, 030701, 2014.
[11] `http://www.nersc.gov`.